

## Interconnection of defect parameters and stress-induced electric signals in ionic crystals

P. Varotsos, N. Sarlis, and M. Lazaridou

*Department of Physics, Solid State Section, University of Athens, Panepistimioupolis Zografos 157 84, Athens, Greece*

(Received 30 October 1997; revised manuscript received 6 April 1998)

Recent experiments in ionic crystals reveal that (in the absence of any external electric field) a time-dependent electric polarization arises upon changing the rate of the uniaxial stress or by the indenter penetration into the crystal surface. The latter experiments lead to activation volumes, which are order(s) of magnitude smaller than those measured by Lazarus and co-workers [Phys. Rev. B **5**, 4935 (1972); Phys. Rev. B **8**, 1726 (1973)]. We show that this difference is not inconsistent with thermodynamical concepts of point defects. Furthermore, an explanation of the nondetection of the cofracture electric signals at large distances, when the crystal is surrounded by a weakly conducting medium, is suggested. [S0163-1829(99)14801-X]

Low-frequency electric signals (i.e., the so-called seismic electric signals) have been reported<sup>1</sup> to precede earthquakes (EQs). These earthquake precursors are detected at certain sites of the surface of the earth lying at distances of the order of 100 km from the focal area(s), while no coseismic (i.e., at the EQ origin time) electric disturbances have been recorded at these sites. The present paper provides an attempt to put the effect on a physical basis by relying on the existing experimental evidence for the prefracture (and cofracture) emission of the electric signals from ionic solids upon changing the applied stress as well as by considering the attenuation of the emitted signals when the solid is surrounded by a weakly conducting medium (as in the case of the earth).

Lazarus and co-workers<sup>2</sup> measured, in ionic crystals, at rather high temperatures, the variation of the ionic conductivity and self-diffusion coefficients upon hydrostatic pressure ( $P$ ). For example, in NaCl they found that the volume  $v^m$  for the cation vacancy migration ( $m$ ) is  $7 \pm 1$  cm<sup>3</sup>/mole (cf. the “molecular” volume which is around 27 cm<sup>3</sup>/mole), while the volume  $v^f$  for the Schottky defect formation is appreciably larger, i.e.,  $55 \pm 9$  cm<sup>3</sup>/mole. Roughly speaking,  $v^m$  is around one-third to one-fourth of the “molecular” volume  $2\Omega$  ( $\Omega$  denotes the mean atomic volume), while  $v^f$  is almost twice  $2\Omega$ .

Recently,<sup>3</sup> the experimental data on the kinetics of indenter penetration into the crystal surface with time, the contact stress under the indenter, and the electric polarization  $P(t)$  have been analyzed at a time resolution of 1 ms, it was shown that the process of the indenter penetration comprises several stages, and the activation parameters at each state have been determined.<sup>3</sup> The low values of activation (act) volumes  $v_{in}^{act}$  and high contact stresses (up to a third of Young’s modulus) indicated the prevalent mass transport in the first  $\sim 10$  ms of the indenter (in) penetration when up to 80% of the depression is formed; for example, the  $P(t)$  data of the first 10 ms of the penetration in NaCl lead to  $v_{in}^{act} \approx 1$  cm<sup>3</sup>/mole, thus indicating<sup>3</sup> the decisive role of point defects in mass transport. At later stages, in which the rate of the decrease of  $P(t)$  vs the time corresponds to appreciably larger relaxation times, i.e.,  $\tau \approx 10$ –100 s or even larger, the activation volume become close to the values  $\geq 10b^3$  (where  $b$  is the Burgers vector), which are characteristic of the dis-

location flow mechanisms (note also that a recent experimentation study<sup>4</sup> in glass and marble—which do not have piezoelectric properties that might complicate the picture—also shows that electrical polarization arises upon mechanical loading with  $\tau$  of the order of 10 s; the charge carriers that participate in this relaxation process are attributed<sup>4</sup> to weakly pinned ions). Independently, our group<sup>5–8</sup> recently measured the appearance of electric polarization in ionic crystals, and in various rocks as well, under the application of uniaxial stress  $\sigma$  and found that the variation of the rate  $d\sigma/dt$  reflects a variation in  $dP(t)/dt$ . (Our laboratory measurements were carried out in room temperature only, and hence did not allow any determination of the activation enthalpy  $h^{act}$ .) Such variations led to the observation<sup>5–8</sup> of low-frequency transient electric signals before fracture (while more intense signals have been detected<sup>5,6</sup> at the time of the fracture, but they are of appreciably higher frequency). This was explained<sup>6,7</sup> on the basis of the charged dislocations model which was suggested<sup>9</sup> for the explanation of the generation of the aforementioned low-frequency electric signals that are detected<sup>1,10</sup> before earthquakes. As for the coseismic signals, we consider that when the emitting source is surrounded by a weakly conducting medium, the high-frequency electric signals—such as the cofracture ones—exhibit stronger attenuation and hence cannot be detected at large distances (the relevant calculation is given in the Appendix).

The aforementioned indenter penetration experiments (in the temperature range  $T = 77$ –300 K)<sup>3</sup> and the method of analysis can be shortly described as follows: The setup with a moving rod mounted on two soft flat springs provides the frictionless translational motion. At the lower end of the rod a standard indenter is mounted. The upper end of the indenter is loaded with various weights. In the initial state, the specimen is brought into contact with the indenter and the switching-off of an electromagnet maintaining the rod allowed for indenter penetration without any initial velocity. To record an electric signal the specimen was placed between two equivalent probes whose potential difference was supplied to the differential input of a wide-band amplifier (with high input resistance) and then onto the plotter or a storage oscillograph; this provided the record of the electric dipole moment acquired by the specimen synchronously with the indenter penetration  $x(t)$ . For  $T = \text{const}$ , the study of the

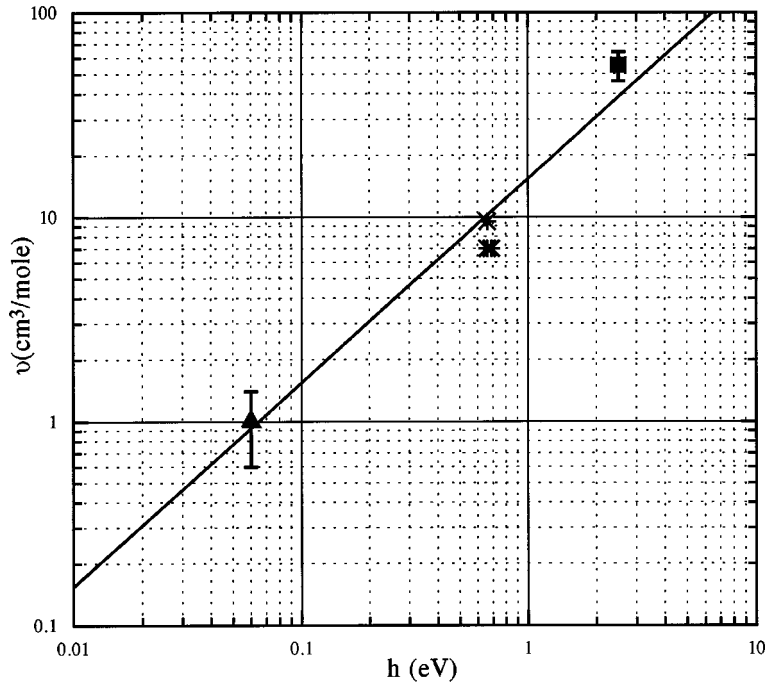


FIG. 1. Experimental point-defect parameters in NaCl. Triangle: microindentation process; stars: cation vacancy migration; square: Schottky defect formation. The straight line corresponds to the prediction of thermodynamics (Ref. 11), i.e.,  $v/h = b(dB/dP - 1)/B_0^{\text{SL}}$ .

plots  $dx(t)/dt$  versus the time  $t$  and  $dP(t)/dt$  versus  $t$ , on a semilogarithmic scale, showed that the loading process consists not of two but of at least five stages; in the first stage (which lasts a few to several ms at room temperature) the rate of loading and polarization increased with time, whereas in the four subsequent stages they both decreased. (The first stage corresponds to the indenter motion with positive acceleration, and the second stage—which has a duration comparable to the first one—corresponds to the negative acceleration.) The linear dependences of the penetration velocity  $dx(t)/dt$  and rate of polarization  $dP(t)/dt$  on time in the semilogarithmic coordinates at stages two to five indicated that the processes are of relaxation character [the  $dx(t)/dt$  and  $dP(t)/dt$  dependences have the same number of stages characterized by close  $\tau_1$  values]. The analysis of the temperature and strength dependences of  $dx(t)/dt$  and  $dP(t)/dt$  yields the activation enthalpy  $h^{\text{act}}$  and the activation volume  $v^{\text{act}}$  for each stage. In the following, we focus our attention on the second stage of the indenter penetration experiments,<sup>3</sup> which seem to be governed by point-defect motion. As an example we consider NaCl.

We first inspect the difference between the volumes that refer to defect motion, i.e.,  $v_{\text{in}}^{\text{act}} = 1 \text{ cm}^3/\text{mole}$  and  $v^m = 7 \pm 1 \text{ cm}^3/\text{mole}$ ; the difference is even larger if we consider that the latter value comes from a least-squares fitting of the  $\ln \sigma$  values above 1 kbar, while if the lower pressure conductivity values are used, we find a somewhat larger  $v^m$  value, i.e.,  $v^m \approx 9.5 \text{ cm}^3/\text{mole}$ , as discussed in p. 293 of Ref. 11. The enthalpy  $h^m$  for the cation vacancy motion ranges between 0.66 and 0.69 eV (see Table 10.7 of Ref. 11), while the activation enthalpy  $h_{\text{in}}^{\text{act}}$  for the microindentation process<sup>3</sup> is 0.06 eV. Thus, we see that  $v^m$  differs from  $v_{\text{in}}^{\text{act}}$  by one order of magnitude, but the same occurs when comparing  $h^m$  and  $h_{\text{in}}^{\text{act}}$ . In other words, the ratio  $v^i/h^i$  remains almost con-

stant, which is consistent with that expected from thermodynamical considerations on point defects<sup>11</sup> when different migration processes take place in the same host crystal; namely,  $v_{\text{in}}^{\text{act}}/h_{\text{in}}^{\text{act}} \approx 17 \times 10^{-3} \text{ kbar}^{-1}$ ,  $v^m/h^m \approx 15 \times 10^{-3} \text{ kbar}^{-1}$ , and hence  $v_{\text{in}}^{\text{act}}/h_{\text{in}}^{\text{act}} \approx v^m/h^m$ , if we consider that  $v_{\text{in}}^{\text{act}}$  values have an uncertainty<sup>3</sup> of  $\sim 40\%$ , while the Yoon and Lazarus data are appreciably more accurate. It is also interesting to note that the enthalpy  $h^f$  for the Schottky defect formation process is around 2.5 eV (see p. 288 of Ref. 11) and hence, if we consider the aforementioned value of  $v^f = 55 \pm 9 \text{ cm}^3/\text{mole}$  found by Lazarus and co-workers, we obtain  $v^f/h^f \approx (23 \pm 4) \times 10^{-3} \text{ kbar}^{-1}$ ; this value is comparable with the values of  $v_{\text{in}}^{\text{act}}/h_{\text{in}}^{\text{act}}$  and  $v^m/h^m$  obtained above, if we take into account the experimental errors and the fact that the  $v^f/h^f$  value was estimated from the high-temperature data of Lazarus and co-workers, while the others correspond to data from lower temperatures.

We now turn to investigate whether  $v_{\text{in}}^{\text{act}}/h_{\text{in}}^{\text{act}}$  is interconnected to the bulk properties. Varotsos and Alexopoulos<sup>11</sup> suggested that (for various processes, e.g., formation or migration)  $v/h = b(dB/dP - 1)/B_0^{\text{SL}}$ , where  $b = \exp \int_0^T \beta dT$  ( $\beta$  is the volume thermal-expansion coefficient),  $B$  is the isothermal bulk modulus, and  $B_0^{\text{SL}}$  denotes the intercept of the linear part of the plot  $B$  versus temperature with the vertical axis. By considering the values<sup>11</sup>  $B_0^{\text{SL}} \approx 284.7 \text{ kbar}$ ,  $dB/dP = 5.35$ , and  $\exp \int_0^{300} \beta dT \approx 1.03$  we find  $v/h \approx 16 \times 10^{-3} \text{ kbar}^{-1}$ . This value, which was derived solely from elastic and thermal data of the bulk material is in satisfactory agreement with the  $v/h$  values of the various processes mentioned above, i.e.,  $v_{\text{in}}^{\text{act}}/h_{\text{in}}^{\text{act}} \approx v^m/h^m \approx v^f/h^f \approx b\{dB/dP - 1\}/B_0^{\text{SL}}$ . The extent of this agreement can be visualized in Fig. 1.

Another important point should be mentioned. The aforementioned value  $v_{\text{in}}^{\text{act}} = 1 \text{ cm}^3/\text{mole}$  corresponds to  $T$

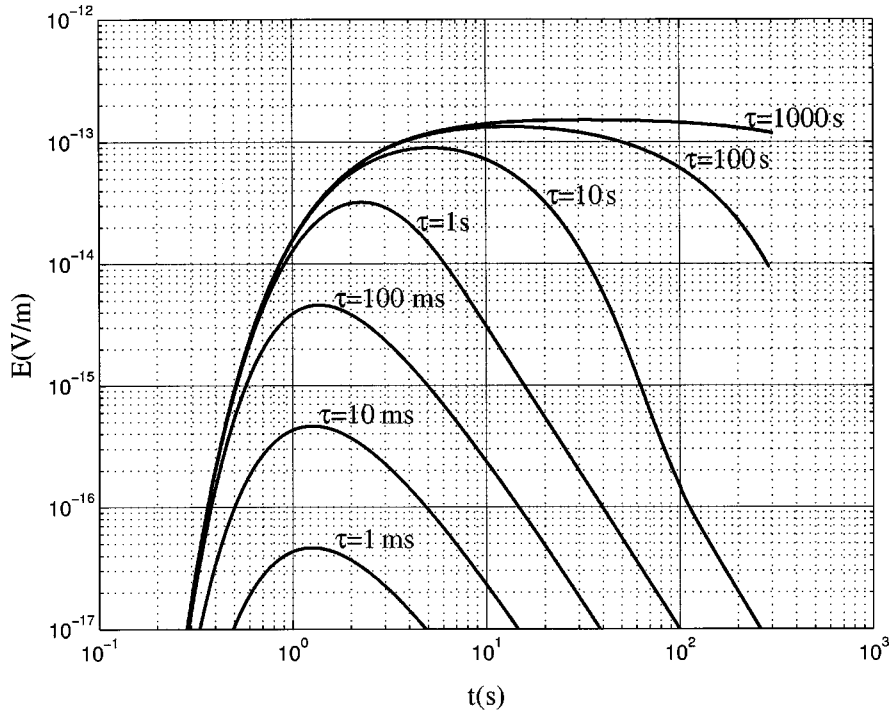


FIG. 2. Amplitude of the electric field (in a medium with  $\sigma = 10^{-3}$  S/m) versus the time, at a distance  $R = 100$  km ( $\theta = 0$ ) from a current dipole source  $I l \exp(-t/\tau)\Theta(t)$ , where  $I l = 1$  A m. The curves correspond to various values of the relaxation time lying between  $\tau = 1$  ms, and 1000 s.

$= 293$  K, while at  $T = 77$  K an appreciably lower value  $v_{\text{in}}^{\text{act}} \approx 0.3$  cm<sup>3</sup>/mole was measured.<sup>3</sup> This temperature dependence of  $v_{\text{in}}^{\text{act}}$  is beyond the experimental error and was also measured for other ionic crystals as well.<sup>3</sup> The fact that the defect volume greatly increases with the temperature (in a way  $v \sim T$ ) was found in Cd and Zn and used by Gilder and Lazarus<sup>12</sup> in order to explain the upwards curvature of the Arrhenius plots. This can be understood on the basis of thermodynamics, if we recall<sup>11</sup> that the defect volume  $v = (dg/dP)_T$  consists of two terms  $v_h = (dh/dP)_T$  and  $v_s = -T(ds/dP)_T$ , where  $g$ ,  $h$ ,  $s$  denote the defect Gibbs energy, enthalpy and entropy, respectively. As  $v = v_h + v_s$ , the thermal-expansion coefficient  $\beta_v$  of the volume  $v$  is given by  $\beta_v = (1/T)v_s/(v_h + v_s)$ , while  $v_s$  is connected to  $\beta_v$  through the relation<sup>11</sup>  $v_s = T v \beta_v$ . By combining these relations, the expansion coefficient  $\beta_s = (1/v_s)(\partial v_s/\partial T)_P$  is found to be<sup>11</sup>

$$\beta_s = (T \partial v / \partial T)^{-1} (T \partial^2 v / \partial T^2 + \partial v / \partial T), \quad \text{for } P = \text{const.}$$

The last relation indicates that  $\beta_s$  is almost equal to  $1/T$  when  $(T \partial^2 v / \partial T^2)_P \ll (\partial v / \partial T)_P$ ; the latter inequality seems to hold in the available experiments up to date, and hence  $\beta_s \sim 1/T$  ( $\approx \beta_v$ ), which implies that  $v$  is almost proportional to  $T$ . The latter could be justified as follows: Recalling that  $s = -(\partial g / \partial T)_P$  and  $v = (\partial g / \partial P)_T$  we can write<sup>11</sup>

$$dg(P, T) = (\partial g / \partial T)_P dT + (\partial g / \partial P)_T dP,$$

$$\text{or } dg = -s dT + v dP,$$

which reveals

$$(\partial v / \partial T)_P = -(\partial s / \partial P)_T.$$

Therefore, in order to justify that  $v \sim T$ , we must alternatively show that  $(\partial s / \partial P)_T \approx \text{const}$ . The pressure dependence of the entropy can be better studied if we consider the simplified expression (see p. 79 of Ref. 11):

$$s = -k \sum_{\alpha=1}^{3N} \ln[\omega'_{\alpha}(V+v)/\omega_{\alpha}(V)],$$

where the frequencies  $\omega'_{\alpha}$  and  $\omega_{\alpha}$  refer to the activated state and the normal state, respectively, and hence to different volumes  $V+v$  and  $V$ . Upon changing pressure the bulk volume  $V$  and the defect volume  $v$  also change, but their compressibilities do not differ by a significant factor (see Chap. 14.2 of Ref. 11) and hence the ratio  $(V+v)/V$  could be roughly considered as constant. As the frequencies do not explicitly depend on temperature (but mainly depend on volume)<sup>11,13</sup> we could argue that, upon changing the pressure, the ratio  $\omega'_{\alpha}(V+v)/\omega_{\alpha}$  remains almost unchanged and hence we may conclude that  $(\partial s / \partial P)_T \approx \text{const}$ . (It is understood that such an explanation fails if the driving mode for the defect activation process depends on volume in a way drastically different than the bulk frequencies, see p. 369 of Ref. 11.)

In summary, indenter penetration experiments<sup>3</sup> (or measurements upon changing the rate of the uniaxial stress<sup>5-8</sup>) in ionic crystals indicate that a time-dependent electric polarization arises (although the crystals are not piezoelectric), which comprises several stages. The early (short duration) stages seem to be governed by point-defect processes, while the later are probably associated with dislocation flow mechanisms. In this paper, we found that, although the defect volumes (and the corresponding enthalpies) studied up to date for various point-defect processes in NaCl, vary by

almost two orders of magnitude, they are interconnected in a way predicted by thermodynamics. An explanation of the experimental result that  $\nu$  increases significantly with temperature was also attempted. Furthermore, we showed that the cofracture electric signals are strongly attenuated when the emitting solid is surrounded by a weakly conducting medium and hence are not detected at large distances.

#### APPENDIX: ATTENUATION OF ELECTRIC SIGNALS IN A CONDUCTING MEDIUM

We first proceed to the investigation in the frequency domain and consider a weakly conducting medium, e.g., with conductivity  $\sigma = 10^{-3}$  S/m. For a frequency  $f \approx 1$  Hz, we find that the effective ‘‘wavelength’’  $\lambda$  is  $\lambda \approx 3$  km and hence the corresponding ‘‘skin depth’’  $\delta (= \lambda/2\pi)$  is around 0.5 km; if we consider a lower frequency, i.e.,  $f = 0.01$  Hz, we find  $\lambda = 1000$  km and hence  $\delta \approx 160$  km (if we take  $f < 0.1$  Hz we find  $\delta > 50$  km). In other words, if measurements are carried out at distances of  $R \approx 100$  km, the low-frequency electric signals exhibit significantly less attenuation than the high-frequency ones.

We now turn to the time domain. We consider a signal emitted from a source with a time dependence of the form  $f(t) = \exp(-t/\tau)\Theta(t)$ , where  $\Theta(t)$  is the Heaviside unit-step function, and we shall determine the amplitude of the signal recorded at long distances, e.g.,  $R \approx 100$  km. For the sake of simplicity, we assume a current dipole source  $IIf(t)$  with a (maximum) dipole moment  $II = 1$  A m. The transient electric field in a medium of conductivity  $\sigma$  due to a current distribution  $\mathbf{j}(\mathbf{r}, t)$  is given by

$$\mathbf{E}(\mathbf{r}, t) = \int \int \int_{V'} \int_{-\infty}^t \mathbf{g}(\mathbf{r}, \mathbf{r}'; t - t') \mathbf{j}(\mathbf{r}', t') d^3 \mathbf{r}' dt', \quad (\text{A1})$$

where  $\mathbf{g}(\mathbf{r}, \mathbf{r}'; t - t')$  is the tensor Green’s function. Assuming a current density of the form  $\mathbf{j}(\mathbf{r}, t) = II \delta^3(\mathbf{r}) f(t) \mathbf{e}_z$ , Eq. (A1) leads, in the quasistatic approximation, to (the dipole is assumed at the origin of a spherical system of coordinates):

$$\begin{aligned} \mathbf{E}(\mathbf{r}, t) = & [\mu/(4\pi^3)^2] [II/(R\tau_0^2)] [\cos(\varphi)\sin(\theta)\cos(\theta)I_{7/2}\mathbf{e}_x \\ & + \sin(\varphi)\sin(\theta)\cos(\theta)I_{7/2}\mathbf{e}_y + (I_{5/2} - \sin^2(\theta)I_{7/2})\mathbf{e}_z], \end{aligned} \quad (\text{A2})$$

where  $\mathbf{e}_x, \mathbf{e}_y, \mathbf{e}_z$ , denote, respectively, the unit vectors along the  $x, y, z$  axis,  $\mu$  is the magnetic permeability of the medium,  $(R, \theta, \phi)$  are the spherical coordinates of  $\mathbf{r}$ ,  $\tau_0 = \mu\sigma R^2/4$ , and  $I_\nu = \int_{-\infty}^t [\tau_0/(t-t')]^\nu \exp[-\tau_0/(t-t')] f(t') dt'$ . The amplitude of the electric field is found from Eq. (A2)

$$\begin{aligned} |\mathbf{E}(\mathbf{r}, t)| = & [\mu/(4\pi^3)^2] \\ & \times [II/(R\tau_0^2)] \sqrt{[I_{5/2}^2 + \sin^2(\theta)I_{7/2}(I_{7/2} - 2I_{5/2})]}. \end{aligned} \quad (\text{A3})$$

Figure 2 depicts the amplitude of the electric field (at  $\theta = 0$ ) for various values of the relaxation time  $\tau$ . An inspection of this figure shows that, for long relaxation times, i.e.,  $\tau \gg \tau_0$  ( $\tau_0 \approx 3$  s if  $\sigma = 10^{-3}$  S/m and  $R = 100$  km), the maximum amplitude of the recorded signal approaches the value expected from the static [i.e., if  $f(t) = 1$ ] calculation<sup>14</sup> (but in the absence of the more conductive paths discussed in Ref. 14); on the other hand, for short relaxation times, i.e.,  $\tau \ll \tau_0$ , the maximum amplitude is smaller by order(s) of magnitude.

- <sup>1</sup>P. Varotsos, K. Alexopoulos, K. Nomicos, and M. Lazaridou, *Nature (London)* **322**, 120 (1986); P. Varotsos, K. Alexopoulos, and M. Lazaridou, *Tectonophysics* **224**, 1 (1993).  
<sup>2</sup>D. N. Yoon and D. Lazarus, *Phys. Rev. B* **5**, 4935 (1972); G. Martin, D. Lazarus, and J. L. Mitchell, *ibid.* **8**, 1726 (1973).  
<sup>3</sup>Yu. I. Golovin and A. I. Tyurin, *Crystallogr. Rep.* **40**, 818 (1995).  
<sup>4</sup>V. S. Kuksenko, Kh. Makhudov, and A. V. Ponomarev, *Fiz. Tverd. Tela (S.- Peterburg)* **39**, 1202 (1997) [*Phys. Solid State* **39**, 1065 (1997)].  
<sup>5</sup>C. Mavromatou and V. Hadjicontis, in *Electromagnetic Phenomena Related to Earthquake Prediction*, edited by M. Hayakawa and Y. Fujinawa (TerraPub, Tokyo, 1994), pp. 293.  
<sup>6</sup>V. Hadjicontis, C. Mavromatou, and Y. Enomoto, in *Materials Science Forum* (Trans Technology, Switzerland, 1997), Vol. 239–241, pp. 435.  
<sup>7</sup>V. Hadjicontis and C. Mavromatou, in *The Critical Review of*

- VAN: Earthquake Prediction from Seismic Electric Signals*, edited by Sir J. Lighthill (World Scientific, Singapore, 1996), pp. 105.  
<sup>8</sup>V. Hadjicontis and C. Mavromatou, *Geophys. Res. Lett.* **21**, 1687 (1994).  
<sup>9</sup>L. Slifkin, *Tectonophysics* **224**, 149 (1993).  
<sup>10</sup>P. Varotsos and M. Lazaridou, *Tectonophysics* **188**, 321 (1991).  
<sup>11</sup>P. Varotsos and K. Alexopoulos, in *Thermodynamics of Point Defects and their Relation with Bulk Properties*, edited by S. Amelinckx, R. Gevers, and J. Nihoul (North-Holland, Amsterdam, 1986).  
<sup>12</sup>H. M. Gilder and D. Lazarus, *Phys. Rev. B* **11**, 4916 (1975).  
<sup>13</sup>P. Varotsos, *Phys. Rev. B* **37**, 6511 (1988).  
<sup>14</sup>P. Varotsos, N. Sarlis, M. Lazaridou, and P. Kaporis, *J. Appl. Phys.* **83**, 60 (1998).